DINAMIKA REKAYASA
http://dinarek.unsoed.ac.id

Volume 21 Nomor 1 (2025) Hal.17-28
e-ISSN 2527-6131
http://jurnaldinarek.id

INOVASI METODE POLIGON TERTUTUP DALAM PERHITUNGAN DIAGRAM INTERAKSI LENTUR BIAXIAL PADA KOLOM BETON BERTULANG BERPENAMPANG BERLUBANG

INTERACTION DIAGRAM OF HOLLOW-CROSSED REINFORCED CONCRETE COLUMNS UNDERGOING BIAXIAL BENDING USING THE CLOSED POLYGON METHOD

Yudi Susetyo*[1], Agus Maryoto[1], dan Nanang Gunawan Wariyatno[1]

*Email: yudisusetyo5@gmail.com

[1] 1. Jurusan Teknik Sipil, Fakultas Teknik Universitas Jenderal Sudirman Purwokerto, Indonesia

***Abstrak*—** Design kolom beton bertulang pada kondisi tertentu dibutuhkan penampang yang berlubang misalnya untuk jalur *plumbing* dan jalur kabel. Penampang ini memerlukan analisis yang lebih cermat. Karena *praktek* perencanaan lebih rumit jika dihitung secara manual. Sehingga penelitian ini bertujuan untuk mengembangkan metode perhitungan analisis yang universal mengenai diagram interaksi kolom berlubang dengan diseminasi program komputer INDCOL (*Interaction Diagram of Concrete Column Section*). Analisis kekuatan kolom menggunakan metode *strain compatibality*. Analisis *properties* penampangnya menggunakan metode geometri poligon-tertutup. Dimana titik-titik simpul poligon penampang diberi label numerik. Penomoran titik-titik simpul *exterior boundary* disusun berurutan mengikuti arah berlawanan jarum jam, sedangkan internal *boundary* disusun berurutan searah putaran jarum jam. Hal pembeda dengan peneliti sebelumnya adalah Pertama, jumlah interior *boundary* yang berdiri sendiri diperkenankan lebih dari satu. Ke-dua, sistem urutan penomoran interior *boundary* harus tersusun searah putaran jarum jam. Hasil perhitungan metode ini dibandingkan dengan hasil hitung program PCA-COL. Adapun hasil uji indeks kinerja NMSE atas 3 sudut putar penampang, masing-masing 00, 300, dan 450. Untuk kapasitas gaya aksial dari ke-3 model diperoleh Indek kinerja NMSE masing-masing; 0,0000212066, 0,0000244858, 0,0000300786. Sedangkan uji indeks kinerja NMSE kapasitas momen lentur ke-3 model masing-masing diperoleh; 0.045109796, 0.048488446, 0.04994925. Semua mendekati nol, sehingga metode perhitungan memiliki akurasi yang tinggi.

Kata kunci— Diagram Interaksi, penampang kolom berlubang, metode poligon tertutup.

Abstract— Designing reinforced concrete columns under specific conditions often requires sections with holes, such as for plumbing or cable pathways. These sections need a more precise analysis, as manual calculations can be more complex. Therefore, this study aims to develop a universal analytical method for the interaction diagram of hollow columns using the INDCOL (Interaction Diagram Of Concrete Column Section) software. The column strength is analyzed using the strain compatibility method, and the section properties are analyzed using a polygonal geometry method. The vertices of the polygonal section are assigned numerical labels. The labeling of exterior boundary points follows a counterclockwise sequence, while the interior boundary points are numbered clockwise. The key differences from previous studies are: first, the number of independent interior boundaries can be more than one, and second, the numbering sequence for interior boundaries must follow a clockwise direction. The results from this method are compared with those from the PCA-COL program. Performance index tests using the NMSE (Normalized Mean Squared Error) for three section rotations (0°, 30°, and 45°) resulted in axial force capacities with NMSE indices of 0.0000212066, 0.0000244858, and 0.0000300786, respectively. The bending moment capacities showed NMSE indices of 0.045109796, 0.048488446, and 0.04994925. All values approach zero, indicating the method's high accuracy.

Keywords— Interaction Diagram, hollow column cross section, closed polygon method.

I. INTRODUCTION

To accommodate cable ducts and pipe systems, a reinforced concrete column was designed with several openings in its cross-section. This design choice introduces additional complexity in the structural strength analysis of the column.

Analyzing the strength of columns with perforated cross-sections generally requires the aid of computer software, as manual calculations become significantly more complex. [1] **Ibraheem (2022) and Helgason (2010)** explain that in the case of a symmetric rectangular column subjected to biaxial bending moments (about both the major and minor axes), the bending no longer occurs along the principal axes. Instead, the plastic neutral axis divides the cross-section into irregular shapes, making the analysis more intricate. Several methods have been proposed to calculate the concrete compression area of perforated column cross-sections. [2]**Fattah et al. (2017)** modeled the cross-section as a mesh consisting of smaller discrete elements, each with its own area and centroidal distance to the plastic axis. [3]**Al-Ansari (2019)** introduced the equivalent square method, whereby irregularly shaped cross-sections under biaxial bending are approximated as equivalent square columns with the same area, simplifying the analysis process.

[4]**Greulich (1995),** [5]**Ranjbaran (1992),** [6] **Kwan & Liauw (1985), and** [7]**Marin (1983)** calculated the area of cross-sections with interior boundaries (holes) by assigning sequential numbers to the nodal points along with their Cartesian coordinates. These coordinates were arranged into a closed polygon format, integrating the interior boundary with the exterior boundary. The nodes of the polygon must be ordered counterclockwise. Through geometric methods, the cross-sectional area and centroid can then be accurately computed.

Some personal computer software such as [8]**PCA-Col (1992)** and [9]**SP-Column (2017)** are capable of analyzing column sections with a single interior boundary, either connected to or independent from the exterior boundary. However, these programs do not support the placement of multiple independent interior boundaries. Similarly, AutoCAD software can compute the area and centroid of sections with interior boundaries integrated with the exterior boundary, but it struggles with independently standing interior boundaries.

This study introduces several innovations that differentiate it from previous research and from the capabilities of software such as AutoCAD, PCA-Col, and SP-Column. **First**, the proposed method allows for more than one independent interior boundary. **Second**, the numbering sequence for the interior boundaries must be arranged in a clockwise direction (as illustrated in Figure 2), which results in negative values to indicate subtraction from the total area. In contrast, the exterior boundary must be numbered counterclockwise, resulting in positive values, indicating additive contributions. This system distinguishes between solid and perforated sections.

To validate the accuracy of the calculated cross-sectional area and centroid, results are compared with AutoCAD outputs. Meanwhile, to verify the interaction diagram calculations, comparisons are made with PCA-Col output. PCA-Col was selected for this purpose due to its manageable number of neutral axis iterations (26 per section), compared to SP-Column, which generates up to 71 iterations per section. Therefore, a new computer program named **INDCOL** was developed to address the limitations of PCA-Col and SP-Column and to better meet user needs.

II. METHODS

A. Determining Concrete and Reinforcement Data

This study analyzes a reinforced concrete column cross-section in the shape of a rectangle with two internal voids, as illustrated in Figure 1. The column will be evaluated under three different biaxial moment conditions, each resulting in a distinct bending direction and corresponding to three different section rotation angles: 0°, 30°, and 45°. For each of these cases, an interaction diagram will be developed.

The classification data used in the analysis include: concrete compressive strength $f'c$=28 MPa, yield strength of reinforcing steel fy=400 MPa, modulus of elasticity of steel Es=200000 kN/mm2, maximum concrete strain εcu= 0,003 mm/mm. Based on this data, the factor $\beta 1$ is determined as $\beta 1$= 0,85. Subsequently, data are compiled regarding the number of boundaries and the number of nodal points for each boundary, along with the X and Y coordinates (Xc, Yc) of these nodes. The exterior boundary nodes are numbered in a counterclockwise direction, while interior boundary nodes are numbered clockwise. ***Pe1*** to ***Pe5*** denote the nodes on the exterior boundary, while ***Pi1*** to ***Pi5*** and ***Pi'1*** to ***Pi'5*** denote the nodes for interior boundaries 1 and 2, respectively. The cross-section used as a case study, shown in Figure 2, is analyzed under the biaxial moment condition at a 30° angle.

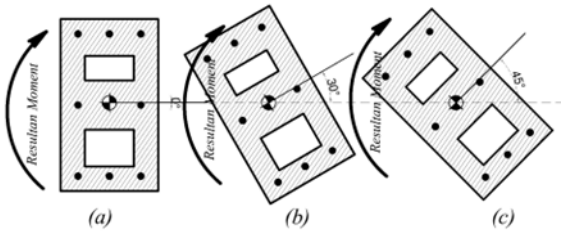

Figure-1. Reinforced concrete column section with three biaxial moment treatment models

Table 1. Coordinates of exterior boundary nodes

Joint	Pe1	Pe2	Pe3	Pe4	Pe5
Xj	3,0964	-343,31	6,6862	353,0964	3,0964
Yj	394,6369	194,637	-411,6	-211,581	394,6369

Table 2. Coordinates of interior boundary 1 nodes

Joint	Pi1	Pi2	Pi3	Pi4	Pi5
Xj	216,4938	43,2888	-31,71	141,4938	216,4938
Yj	-174,978	-274,97	-145,1	-45,0745	-174,978

Table 3. Coordinates of interior boundary 2 nodes

Joint	Pi'1	Pi'2	Pi'3	Pi'4	Pi'5
Xj	41,4938	-131,71	-181,711	-8,5062	41,4938
Yj	128,130	28,1306	114,7331	214,7331	128,1306

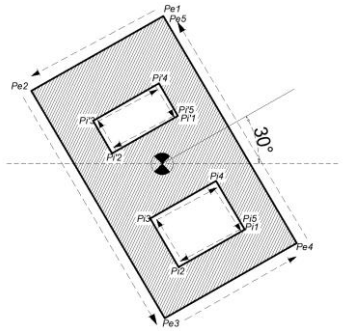

Figure-2. Numbering sequence of nodal points for perforated column section boundaries

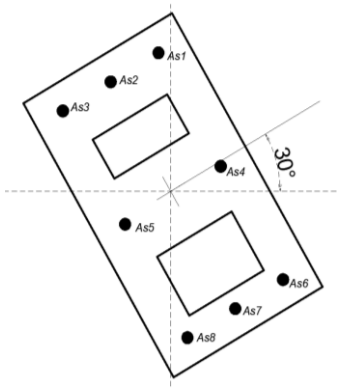

Figure-3. Coordinates of individual reinforcement bars

Based on Figure 3, the coordinates and areas of the reinforcement bars (***Xs, Ys* and *As***) are listed in Table 4 below.

Table 4. Coordinates and area of each reinforcement bar

No. As	Xs (mm)	Ys(mm)	As(mm2)
As1	-28,8527	306,9091	605,1375
As2	-140,1087	242,6754	605,1375
As3	-251,3647	178,4417	605,1375
As4	116,1473	55,7618	605,1375
As5	-106,3648	-72,7056	605,1375
As6	261,1474	-195,3857	605,1375
As7	149,8914	-259,6194	605,1375
As8	38,6353	-323,8531	605,1375

B. Calculation of Area and Centroid of the Cross-Section

Among the four methods proposed by **Greulich (1995)** [4], **Ranjbaran (1992)** [5]**, Kwan & Liauw (1985)** [6]**, and Marin (1983)** [7], a slight modification to the formula is adopted in this study. This adjustment is necessary because the previous researchers modeled the interior and exterior boundaries as a single, unified boundary. In contrast, the cross-section considered here consists of multiple independent polygonal boundaries. Therefore, a slightly modified formulation is applied to calculate the area and centroid of the section, while still yielding consistent results. The formulas are as follows:

$$\boldsymbol{Ac} = \sum_{i=1}^{n} \boldsymbol{Api} \quad (1)$$

$$\boldsymbol{Api} = \frac{1}{2((x_i.y_{i+1})-(x_{i+1}.y_i))} \quad (2)$$

$$\boldsymbol{xc} = \frac{1}{\boldsymbol{Ac}} \sum_{i=1}^{n} \frac{1}{3} \boldsymbol{Api}(x_i + x_{i+1}) \quad (3)$$

$$\boldsymbol{yc} = \frac{1}{\boldsymbol{Ac}} \sum_{i=1}^{n} \frac{1}{3} \boldsymbol{Api}(y_i + y_{i+1}) \quad (4)$$

$$\boldsymbol{Act} = \sum_{i=1}^{nb} \boldsymbol{Aci} \quad (5)$$

$$\boldsymbol{Xc} = \frac{1}{\boldsymbol{Act}} \sum_{i=1}^{nb} \boldsymbol{Ac}.\boldsymbol{xc} \quad (6)$$

$$\boldsymbol{Yc} = \frac{1}{\boldsymbol{Act}} \sum_{i=1}^{nb} \boldsymbol{Ac}.\boldsymbol{yc} \quad (7)$$

Where:

Act is the total cross-sectional area obtained by summing the individual areas ***Ac***of ***n*** boundary polygons, ***Aci*** represents the area of the ***i*** -th boundary polygon, ***Xc*** and ***Yc*** denote the x- and y-coordinates, respectively, of the centroid of the entire cross-sectional area ***Act***, ***xc***(i…n) represent the x- and y-coordinates of the centroid of each individual ***i***-th

boundary polygon, ***nb*** refers to the number of closed boundary polygons.

C. Calculation of Concrete Compressive Force Cc and Moment Mc

Changing the position of the neutral axis ***C*** alters both the area of the concrete in compression and the stress distribution in the reinforcement bars. These changes influence the column's moment and axial load capacity. For each iteration step of the neutral axis ***C***, a new boundary polygon is formed, which corresponds to the concrete region above the line x=a, where ***a*** = ***C.β1***. The coordinates of the vertices forming this new shaded boundary are then rearranged. The shaded ***Act*** and its centroid ***Yc*** are calculated using Equations (1) through (7).

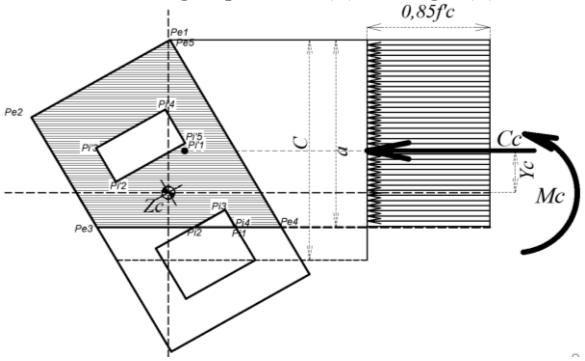

Figure 4. Node numbering for each boundary under a given value of C, along with Cc and Mc

Using Yc as the moment arm of the shaded area and ***Ac*** as the compressive concrete area, the concrete compressive force is calculated as:

$$Cc = 0.85.f'c.Act \quad (9)$$

Where:

Cc represents the compressive force capacity of the concrete cross-section at a height ***a***, while ***Mc*** denotes the resisting moment of the column's centroidal section due to the compressive force ***Cc*** measured relative to the plastic centroid of the column section located at height ***Yc***. This relationship is expressed as follows:

$$Mc = 0.85\,.f'c.Act\,.Yc \quad (10)$$

D. Calculation of Steel Reinforcement Force Cs and Moment Ms

The next dataset includes the number of reinforcement points along with the corresponding coordinates ***Xs*** and ***Ys***, as well as the cross-sectional area ***As*** of each reinforcing bar. To determine the strain in the reinforcement based on a specified neutral axis depth ***C***, a reinforcement strain diagram is obtained. As illustrated in Figure 4, the steel strain varies linearly with the depth of the neutral axis ***C***. The strain ***εs*** at a specific location is calculated using the following strain distribution equation [10]**(K. Wight, 2016)**:

$$\varepsilon si = \left(\frac{C - di}{C}\right) 0,003 \quad (11)$$

$$Cs = \sum_{i=1}^{n} As(f's - 0,85\, f'c) \quad (12)$$

Where ***εsi*** is the strain in the iii-th layer of reinforcing steel at a depth ***di*** from the topmost fiber of the concrete in compression, and ***C*** is the distance from the top fiber to the neutral axis. The stress in the compression reinforcement (as shown in Figure 6) is given by the strain ***εs*** multiplied by the modulus of elasticity of the steel ***Es,*** and must not exceed the yield stress ***fy***. Since steel behaves elastically until it reaches the yield strain ***εy***, if the compressive strain in the reinforcement ***εs′*** equals or exceeds ***εy***, then the stress ***f***s' is limited to the yield stress ***fy***. The steel stress ***fs*** is thus given by:

$$f's = Es\,\varepsilon's\,, -fy \le fsi\,fy \quad (13)$$

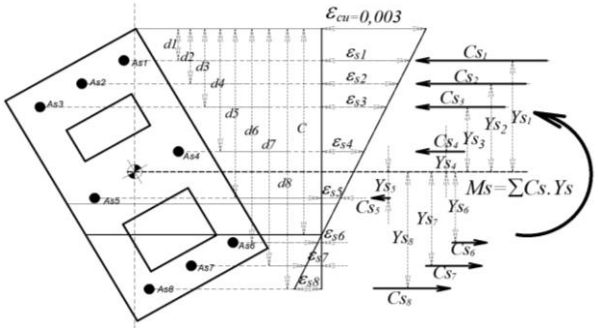

Figure 5. Stress diagram for a given value of ***C,*** illustrating ***Cs*** and ***Ms***

If the height ***a*** exceeds the depth of a given reinforcing layer from the top concrete fiber, then the area of reinforcement in that layer is included in the compression concrete area used to calculate ***Cc***. Therefore, the value of ***f's*** for that layer is reduced by ***0,85 f'c***. Before computing ***Cs***, any positive ***f's must*** be reduced by ***0,85. f'c***. Hence, the axial force in the compression reinforcement is expressed as:

$$Cs = \sum_{i=1}^{n} As\, fs + \sum_{i=1}^{n} As(f's - 0,85\, f'c) \quad (14)$$

The resisting moment of the column section due to both tensile and compressive reinforcement,

measured relative to the plastic centroid of the column, is calculated as follows:

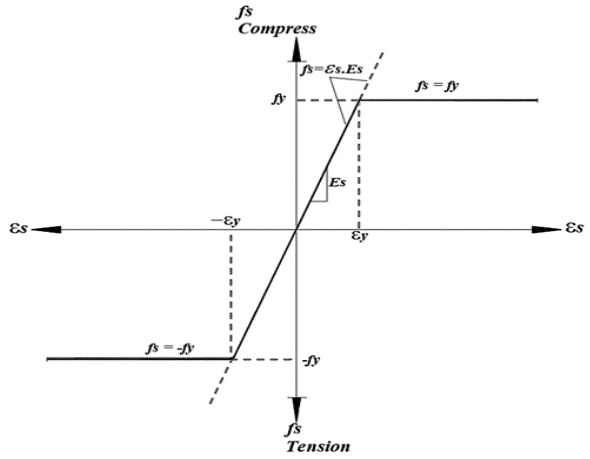

Figure 6. Stress-strain diagram for reinforcing steel

$$\boldsymbol{Ms} = \sum_{i=1}^{n} \boldsymbol{Cs}\,.\ \boldsymbol{ys} + \sum_{i=1}^{n} \boldsymbol{As}(\boldsymbol{f's} - \mathbf{0,85}\,\boldsymbol{f'c}).\boldsymbol{ys} \quad (15)$$

Where ***n*** is the number of reinforcement layers, ***Cs*** is the axial force due to steel reinforcement, ***As*** is the area of reinforcement in the ***i***-th layer, ***f's*** is the compressive stress in the steel (equal to ***ε's·Es)*** and ***Ys*** is the distance from each reinforcing bar to the plastic ***X***-axis. The unfactored axial load capacity of the column is calculated as:

$$\boldsymbol{Pn} = \boldsymbol{Cc} + \boldsymbol{Cs} \quad (16)$$

The corresponding unfactored bending moment capacity of the column is:

$$\boldsymbol{Mn} = \boldsymbol{Mc} + \boldsymbol{Ms} \quad (17)$$

After performing several iterations on the neutral axis ***C***, starting from a height three times the section depth down to the top compression fiber, and dividing the depth into 26 increments, the factored capacities ***ϕ Pn*** and ***ϕ Mn*** are calculated. These values are then plotted on a Cartesian graph to form a curve resembling half an onion clove, known as the Interaction Diagram for Reinforced Concrete Columns.

E. Model Validation

To evaluate the accuracy of the manual calculations compared to the PCA-Col software output, the calculated values of ***ϕ Pn*** and ***ϕ Mn*** were compared to those generated by PCA-Col. According to **Poli & Cirillo (1993)** [11]**,** the performance index NMSE (Normalized Mean Square Error) is used to assess the level of coherence between the manual calculations and the PCA-Col results:

$$\text{NMSE} = \sum Si^2(1-ki)^2 \,/\, \sum Si\ ki \quad (18)$$

Where ***Si=Co/avg(Co),*** and ***ki=Co/Ca,*** being the predicted value and ***Co*** the evaluated (actual) value. Each value represents the observed and predicted axial force or moment

III. RESULT AND DISCUSSION

The calculation of the cross-sectional area and centroid ***Zc*** is the initial step in determining the location of the plastic centroid of the concrete column section, which is assumed to be at coordinates ***x=0*** and ***y=0***. Based on Table 1, Table 2, Table 3, and Figure 2, the area and centroid of the section are calculated as follows:

A. Cross-sectional Area Ac

$$\boldsymbol{Ace} = \frac{1}{2}\big((x_1.y_2) - (x_2.y_1)\big) + \frac{1}{2}\big((x_2.y_3) - (x_3.y_2)\big) +$$

$$\tfrac{1}{2}\big((x_3.y_4) - (x_4.y_3)\big) + \tfrac{1}{2}\big((x_4.y_5) - (x_5.y_4)\big)$$

$$\boldsymbol{Ace} = \frac{1}{2}\big((3{,}0964\,.\,194{,}6369) - (-343{,}3138\,.\,394{,}6369)\big)$$

$$+\tfrac{1}{2}\big((-343{,}3138\,.\,-411{,}5809) + (6{,}6862\,.\,194{,}6369)\big)$$

$$+\tfrac{1}{2}\big((6{,}6862\,.\,-211{,}5809) + (353{,}0964\,.\,-411{,}5809)\big)$$

$$+\tfrac{1}{2}\big((353{,}0964\,.\,394{,}6369) - (3{,}0964\,.\,-211{,}5809)\big)$$

$$\boldsymbol{Ace} = 68043{,}48373 + 70000{,}01077 + 71956{,}53094 + 70000$$

$$\boldsymbol{Ace} = 280000\ mm^2$$

B. X-Coordinate of the Centroid Xc of the Exterior Boundary

$$\boldsymbol{xce} = \frac{1}{Ac}\big[\frac{1}{3}Ap1(x_1 + x_2) + \frac{1}{3}Ap2(x_2 + x_3) + \frac{1}{3}Ap3(x_3 + x_4)$$

$$+\frac{1}{3}Ap4(x_4 + x_5)\big]$$

$$\boldsymbol{xce} = \tfrac{1}{280000}\big[\tfrac{1}{3}68043{,}48.(3{,}0964\text{-}343{,}3138) + \tfrac{1}{3}70000{,}01.(\,\text{-}343{,}3138 +$$

$$6{,}6862) + \tfrac{1}{3}71956{,}53.(\,6{,}6862 + 353{,}0964) +$$

$$\tfrac{1}{3}70000(353{,}0964 + 3{,}0964)\,\big]$$

C. Y-Coordinate of the Centroid Yc of the Exterior Boundary

$$\boldsymbol{yce} = \frac{1}{Ac}\big[\frac{1}{3}Ap1(y_1 + y_2) + \frac{1}{3}Ap2(y_2 + y_3) + \frac{1}{3}Ap3(y_3 + y_4)$$

$$+\frac{1}{3}Ap4(y_4 + y_5)\big]$$

$$\boldsymbol{yce} = \tfrac{1}{280000}\big[\tfrac{1}{3}68043{,}48.(394{,}6369 + 194{,}6369) +$$

$$\tfrac{1}{3}70000{,}01.(194{,}6369 - 411{,}5809)$$

$$+\tfrac{1}{3}71956{,}53.(\text{-}411{,}5809 - 211{,}5809) + \tfrac{1}{3}70000(\text{-}211{,}5809 + 394{,}6369)\,\big]$$

$$\boldsymbol{yce} = \frac{1}{280000}[13365414{,}07392 - 5062027{,}4457$$

$$- 14946853{,}781$$

$+4271306{,}9045 - 2372160{,}243]$

$\boldsymbol{yce = -8{,}4720}$ **mm**

D. Area of Interior Boundary (Void 1)

$$\boldsymbol{ci1} = \frac{1}{2}\left((x_1.y_2) - (x_2.y_1)\right) + \frac{1}{2}\left((x_2.y_3) - (x_3.y_2)\right)$$

$$+\tfrac{1}{2}\left((x_3.y_4) - (x_4.y_3)\right) + \tfrac{1}{2}\left((x_4.y_5) - (x_5.y_4)\right)$$

$$\boldsymbol{Aci1} = \frac{1}{2}\left((216{,}4938\,.-274{,}9783) - (43{,}2888\,.-174{,}9783)\right)$$

$$+\tfrac{1}{2}\left((43{,}2888\,.-145{,}0745) - (-31{,}7112\,.-274{,}9783)\right)$$

$$+\tfrac{1}{2}\left((-31{,}7112\,.-45{,}0745) - (141{,}4938\,.-145{,}0745)\right)$$

$$+\tfrac{1}{2}(-145{,}0745\,.-174{,}9783) - (216{,}4938\,.-45{,}07459))$$

$$\boldsymbol{Aci1} = -25978{,}24823 - 7499{,}99644 + 10978{,}25439 - 7499{,}9974$$

$\boldsymbol{Aci1 = -29999{,}98768}$ *mm*^{2}

E. X-Coordinate of the Centroid Xc of Void 1

$$\boldsymbol{xci1} = \frac{1}{Ac}[\frac{1}{3}Ap1(x_1 + x_2) + \frac{1}{3}Ap2(x_2 + x_3) + \frac{1}{3}Ap3(x_3 + x_4)$$

$$+\frac{1}{3}Ap4(x_4 + x_5)]$$

$$\boldsymbol{xci1} = \tfrac{1}{\boldsymbol{-29999{,}98}}[\tfrac{1}{3} - 25978{,}24823\ (216{,}4938 + 43{,}2888)$$

$$+\tfrac{1}{3} - 7499{,}99644\ (43{,}2888 - 31{,}7112)$$

$$+\tfrac{1}{3}10978{,}25439\ (-31{,}7112 + 141{,}4938)$$

$$+\ \tfrac{1}{3} - 7499{,}9974(141{,}4938 + 216{,}4938)]$$

$$\boldsymbol{xci1} = \tfrac{1}{\boldsymbol{-29999{,}98}}[-2249565{,}62251 - 28943{,}98627 + 401740{,}43666 -$$

$$894968{,}68953]$$

$\boldsymbol{xci1 = 92{,}39130}$ **mm**

F. Y-Coordinate of the Centroid Yc of Void 1

$$\boldsymbol{yci1} = \frac{1}{Ac}[\frac{1}{3}Ap1(y_1 + y_2) + \frac{1}{3}Ap2(y_2 + y_3) + \frac{1}{3}Ap3(y_3 + y_4)$$

$$+\frac{1}{3}Ap4(y_4 + y_5)]$$

$$\boldsymbol{yci1} = \tfrac{1}{\boldsymbol{-29999{,}98}}[\tfrac{1}{3}.-25978{,}24823\ (-174{,}9783 - 274{,}9783)$$

$$+\tfrac{1}{3} - 7499{,}99644\ (-274{,}9783 - 145{,}0745)$$

$$+\tfrac{1}{3}10978{,}25439\ (-145{,}0745 - 45{,}0745)$$

$$+\ \tfrac{1}{3} - 7499{,}9974(-45{,}0745 - 174{,}9783)]$$

$$\boldsymbol{yci1} = \frac{1}{-29999{,}98}[3896361{,}41520 + 1050131{,}501 - 695834{,}69$$

$$+550131{,}809]$$

$\boldsymbol{yci1 = -160{,}0264}$ **mm**

G. Area of Interior Boundary (Void 2)

$$\boldsymbol{Aci2} = \frac{1}{2}\left((x_1.y_2) - (x_2.y_1)\right) + \frac{1}{2}\left((x_2.y_3) - (x_3.y_2)\right)$$

$$+\tfrac{1}{2}\left((x_3.y_4) - (x_4.y_3)\right) + \tfrac{1}{2}\left((x_4.y_5) - (x_5.y_4)\right)$$

$$\boldsymbol{Aci2} = \frac{1}{2}\left((41{,}4938\,.28{,}1306) - (-131{,}7112\,.128{,}1306)\right)$$

$$+\tfrac{1}{2}\left((-131{,}7112\,.114{,}7331) - (-181{,}7112\,.28{,}1306)\right)$$

$$+\tfrac{1}{2}\left((-181{,}7112\,.214{,}7331) - (-8{,}5062\,.114{,}7331)\right)$$

$$+\tfrac{1}{2}\left((-8{,}5062\,.128{,}1306) - (41{,}4938\,.214{,}7331)\right)$$

$$\boldsymbol{Aci2} = 9021{,}74 - 4999{,}995 - 19021{,}733 - 4999{,}998$$

$\boldsymbol{Aci2 = -19999{,}986}$ *mm*^{2}

H. X-Coordinate of the Centroid Xc of Void 2

$$\boldsymbol{xci2} = \frac{1}{Ac}\left[\frac{1}{3}Ap1(x_1 + x_2) + \frac{1}{3}Ap2(x_2 + x_3) + \frac{1}{3}Ap3(x_3 + x_4)\right.$$

$$\left.+\frac{1}{3}Ap4(x_4 + x_5)\right]$$

$$\boldsymbol{xci2} = \tfrac{1}{-19999{,}986}[\tfrac{1}{3}\ 9021{,}74(41{,}4938\text{-}131{,}7112) + \tfrac{1}{3}\text{-}\ 4999{,}995(\text{-}$$

$$131{,}7112\text{-}181{,}7112)$$

$$+\tfrac{1}{3} - 19021{,}733(\text{-}181{,}7112\text{-}8{,}5062) + \tfrac{1}{3}\text{-}4999{,}998(\text{-}8{,}5062\text{+}41{,}4938)]$$

$$\boldsymbol{xci2} = \tfrac{1}{-19999{,}986}[-271305{,}984 + 522370{,}102 + 1206088{,}217 - 54979{,}316]$$

$\boldsymbol{xci2 = -70{,}1087}$ **mm**

I. Y-Coordinate of the Centroid Yc of Void 2

$$\boldsymbol{yci2} = \frac{1}{Ac}[\frac{1}{3}Ap1(y_1 + y_2) + \frac{1}{3}Ap2(y_2 + y_3) + \frac{1}{3}Ap3(y_3 + y_4)$$

$$+\frac{1}{3}Ap4(y_4 + y_5)]$$

$$\boldsymbol{yci2} = \tfrac{1}{-19999{,}986}[\tfrac{1}{3}\ 9021{,}74(128{,}1306 + 28{,}1306)$$

$$+\tfrac{1}{3}\text{-}\ 4999{,}995(28{,}1306 + 114{,}7331)$$

$$+\tfrac{1}{3} - 19021{,}733(114{,}7331 + 214{,}7331)$$

$$+\tfrac{1}{3}\text{-}4999{,}998(214{,}7331 + 128{,}1306)]$$

$$\boldsymbol{yci2} = \tfrac{1}{-19999{,}986}[469915{,}988 - 238105{,}909 - 2089006{,}062 - 571439{,}318]$$

***yci2* = 121,43185 mm**

J. Total Cross-sectional Area of the Column

$$\boldsymbol{Act} = \sum_{i=1}^{nb} \boldsymbol{Ac\ i}$$

Act = *Ace + Aci1 +Aci2*

Act = 280000 mm^2 − 29999,98768 mm^2 −19999,986 mm^2

Act = **230000,02632 mm^2**

K. X-Coordinate of the Overall Section Centroid Xct

$$\boldsymbol{Xct} = \frac{\boldsymbol{1}}{\boldsymbol{Act}}\sum_{i=1}^{nb} \boldsymbol{Ac.xc}$$

$$\boldsymbol{Xct} = \tfrac{1}{230000}\ [\ (280000\ .\ 4{,}8913) + (\ -29999{,}98768.\ 92{,}3913\ ) + (\text{-}$$

$$19999{,}986\ .\ \text{-}70{,}1087)]$$

Xct = 0,000003 mm

L. Y-Coordinate of the Overall Section Centroid Yct

$$Yct = \frac{1}{Act}\sum_{i=1}^{nb} Ac.yc$$

$$Yct = \frac{1}{230000}\ [\ (280000.\ -8{,}472) + (-29999{,}98768.\text{-}160{,}0264) + (\text{-}19999{,}986.\ 121{,}43185)]$$

$$Yct = 0{,}000024\ mm$$

Once the total area and centroid of the section have been determined, the plastic axis of the section is placed at the coordinate ***Zc(0,0)***. Subsequently, the method of calculating area and centroid, as demonstrated previously, is repeated for all iterations corresponding to changes in the coordinates of the nodal points in the shaded section resulting from shifts in the neutral axis ***Cnet***. The neutral axis depth varies from minus three times the height of the section up to the extreme compression fiber, at which point the concrete compression area becomes zero. The results of these computations are presented in Table 10, which shows the axial forces and bending moments derived both from manual calculations and PCA-Col outputs.

M. Calculation of ϕPn & ϕMn for Each Iteration of the Neutral Axis Depth C

Table 9. ϕPn and ϕMn at Bending Angle 0°

			/Perhit manual\		/ PCACOL\	
C-net	Ac	Yc	Pn	Mn	Pn	Mn
1920	230,00	0	7295,22	-17,82	7295,22	-17,82
998,51	230,00	0	6947,67	82,76	6930,46	82,76
807,14	224,43	8,76	6589,16	179,76	6565,7	187,83
769,38	211,59	29,303	6225,77	293,39	6200,94	300,36
731,85	198,83	50,296	5858,67	397,93	5836,18	403,9
684,78	186,41	71,299	5473,81	496,11	5471,42	498,51
622,8	175,88	88,481	5128,00	567,94	5106,66	569,64
568,08	166,57	102,688	4759,47	637,37	4741,9	638,54
521,81	157,42	115,682	4393,02	696,68	4377,13	698,23
490,81	146,88	130,453	4027,03	744,89	4012,37	745,98
461,12	136,78	144,83	3661,98	788,10	3647,61	788,77
432,71	127,12	158,848	3296,64	827,32	3282,85	827,66
405,6	117,90	172,523	2930,33	863,51	2918,09	863,56
377,59	108,38	187,035	2560,51	891,28	2553,33	891,06
338,88	95,22	207,951	2199,18	880,56	2188,57	880,04
304,16	83,41	227,909	1832,62	862,60	1823,81	861,88
258,96	74,02	244,368	1463,26	842,08	1459,04	841,63
216,36	66,78	255,88	1097,65	820,15	1094,28	819,66
161,19	54,80	271,712	734,66	756,34	729,52	755,39
128,63	43,73	285,55	368,55	670,39	364,76	669,53
100,79	34,27	297,382	2,93	576,39	0	575,64
77,27	26,27	307,378	-384,77	470,73	-387,29	470,11
58,21	19,79	315,478	-772,74	361,64	-774,58	361,17
46,29	15,74	320,544	-1158,31	252,10	-1161,87	251,64
37,78	12,85	324,161	-1545,19	142,01	-1549,15	141,71
0	0,00	301,362	-1936,44	18,94	-1936,44	18,94

Table-10. ϕPn and ϕMn at Bending Angle 30°

			/Perhit manua		/ PCACOL\	
C-net	Ac	Yc	Pn	Mn	Pn	Mn
2155,47	230,00	0,00	7295,22	-15,43	7295,22	-15,43
1057,02	230,00	0,00	6944,60	71,05	6930,46	71,05
862,43	223,82	10,02	6587,56	165,97	6565,7	169,58
801,83	212,06	27,80	6219,43	269,85	6200,94	274,67
755,46	199,79	45,90	5850,45	362,63	5836,18	366,89
709,97	187,60	63,71	5489,48	440,58	5471,42	443,85
661,63	176,78	79,19	5128,67	509,24	5106,66	511,08
610,49	166,25	93,42	4757,43	565,09	4741,9	566,62
571,49	155,73	106,96	4400,37	609,13	4377,13	610,47
538,8	144,96	120,62	4028,98	647,89	4012,37	648,92
510,77	134,34	134,20	3665,85	679,11	3647,61	679,78
484,11	123,87	147,92	3299,88	705,49	3282,85	705,74
457,45	113,41	162,09	2934,69	727,42	2918,09	727,32
433,34	103,94	175,39	2571,29	744,11	2553,33	743,72
406,81	94,02	189,95	2199,90	748,59	2188,57	747,98
377,89	84,54	204,43	1832,55	744,12	1823,81	743,39
344,28	75,28	218,85	1463,68	726,69	1459,04	725,95
304,67	66,21	232,57	1101,20	693,60	1094,28	692,75
271,22	57,33	245,29	737,88	651,47	729,52	650,36
240,46	47,52	259,28	371,92	590,36	364,76	589
213,34	37,97	273,75	6,36	523,76	0	522,4
183,53	28,10	290,64	-382,92	440,88	-387,29	439,74
152,67	19,45	308,12	-771,23	348,16	-774,58	347,27
121,78	12,37	325,63	-1160,73	250,22	-1161,87	249,62
86,68	6,27	345,52	-1549,59	140,89	-1549,15	140,55
0	0,00	0,00	-1936,44	16,41	-1936,44	16,41

Table 11. ϕPn and ϕMn at Bending Angle 45°

			/Perhit. Manual\		/ PCACOL\	
C-net	Ac	Yc	Pn	Mn	Pn	Mn
2054,43	230,00	0,00	7295,23	-12,60	7295,22	-12,60
984,76	230,00	0,00	6945,46	61,25	6930,46	61,25
815,41	222,82	10,93	6588,47	151,88	6565,7	155,02
755,78	211,67	26,47	6223,36	240,83	6200,94	244,70
706,97	199,97	42,03	5850,92	320,37	5836,18	323,53
660,27	188,74	56,38	5495,15	383,25	5471,42	385,66
615,54	177,94	69,53	5124,74	439,88	5106,66	441,76
576,00	166,82	82,41	4759,85	485,24	4741,9	486,87
544,09	156,20	94,38	4400,73	522,89	4377,13	524,21
515,94	145,62	106,21	4038,85	552,85	4012,37	553,82
488,92	134,38	118,85	3668,37	576,74	3647,61	577,33
464,53	123,33	131,57	3302,07	595,06	3282,85	595,28
442,37	112,87	144,08	2935,09	609,64	2918,09	609,52
420,07	103,00	156,42	2568,57	621,30	2553,33	620,90
396,23	93,24	169,14	2201,66	624,62	2188,57	624,01
371,29	83,90	181,77	1835,75	621,04	1823,81	620,28
345,72	74,68	194,68	1466,17	610,46	1459,04	609,52
320,07	65,54	208,02	1102,39	590,38	1094,28	589,35
292,35	56,61	221,68	736,81	565,19	729,52	564,18
258,83	46,53	237,69	370,99	514,87	364,76	513,80
229,25	37,64	252,60	5,64	456,62	0	455,52
201,16	29,24	268,00	-382,37	390,74	-387,29	389,68
173,55	21,76	283,65	-771,39	321,75	-774,58	320,86
136,15	13,39	304,84	-1160,13	232,36	-1161,87	231,74
92,12	6,13	329,79	-1551,96	130,46	-1549,15	130,15
0,00	0,00	0,00	-1936,44	13,39	-1936,44	13,40

From Table 9, the results are plotted in Figure 8, where the rightmost graph shows two overlapping interaction curves—one from manual calculations and the other from PCA-Col—for a rotation angle of 0°. From Table 10, the data are plotted in the same figure, with the middle graph showing the interaction curves for a rotation angle of 30°. Likewise, Table 11 results are plotted as the leftmost graph in Figure 8, representing the interaction curves for a rotation angle of 45°.

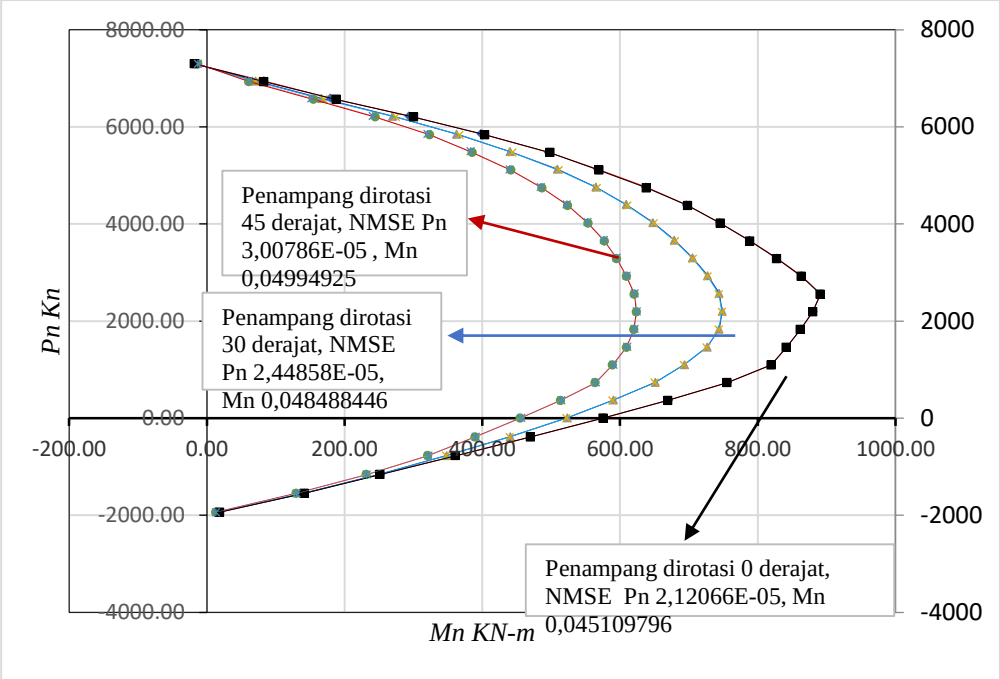

Figure 8. Comparison of Interaction Diagrams between Manual Calculations and PCA-Col Results for the Three Sections at Rotation Angles of 0°, 30°, and 45°, as illustrated in Figure 1.

N. NMSE Performance Index Evaluation

Table-12. NMSE Performance Index Evaluation for Axial Load at 0° Rotation

No.	Pn PCACOL (kN)	Pn CALC (kN)	NMSE C_a/C_o	si	Ki	si^2	si*ki	$(1-ki)^2$	$si^2 * (1-ki)^2$
1	7295,22	7295,22	1,000	2,679	1,000	7,179	2,679	3,00638E-13	2,158324E-12
2	6930,46	6947,67	1,005	2,545	1,002	6,479	2,552	6,16326E-06	3,993293E-05
3	6565,70	6589,16	1,007	2,411	1,004	5,815	2,420	1,27699E-05	7,425833E-05
4	6200,94	6225,77	1,008	2,277	1,004	5,187	2,287	1,60287E-05	8,314002E-05
5	5836,18	5858,67	1,008	2,144	1,004	4,595	2,152	1,48472E-05	6,821789E-05
6	5471,42	5473,81	1,001	2,010	1,000	4,038	2,010	1,90967E-07	7,711800E-07
7	5106,66	5128,00	1,008	1,876	1,004	3,518	1,883	1,74612E-05	6,142494E-05
8	4741,90	4759,47	1,007	1,742	1,004	3,033	1,748	1,37352E-05	4,166178E-05
9	4377,13	4393,02	1,007	1,608	1,004	2,584	1,613	1,31827E-05	3,407070E-05
10	4012,37	4027,03	1,007	1,474	1,004	2,172	1,479	1,33427E-05	2,897626E-05
11	3647,61	3661,98	1,008	1,340	1,004	1,795	1,345	1,55234E-05	2,786126E-05
12	3282,85	3296,64	1,008	1,206	1,004	1,454	1,211	1,76490E-05	2,565781E-05
13	2918,09	2930,33	1,008	1,072	1,004	1,149	1,076	1,75847E-05	2,019895E-05
14	2553,33	2560,51	1,006	0,938	1,003	0,879	0,940	7,90302E-06	6,950300E-06
15	2188,57	2199,18	1,010	0,804	1,005	0,646	0,808	2,35145E-05	1,519331E-05
16	1823,81	1832,62	1,010	0,670	1,005	0,449	0,673	2,33143E-05	1,046113E-05
17	1459,04	1463,26	1,006	0,536	1,003	0,287	0,537	8,34863E-06	2,397432E-06
18	1094,28	1097,65	1,006	0,402	1,003	0,162	0,403	9,50325E-06	1,535062E-06
19	729,52	734,66	1,014	0,268	1,007	0,072	0,270	4,96833E-05	3,566826E-06
20	364,76	368,55	1,021	0,134	1,010	0,018	0,135	1,08220E-04	1,942317E-06
21	0,00	2,93	0,000	0,000	0,000	0,000	0,000	1,00000E+0 0	0,000000E+00
22	-387,29	-384,77	0,987	-0,142	0,993	0,020	-0,141	4,24786E-05	8,594877E-07
23	-774,58	-772,74	0,995	-0,284	0,998	0,081	-0,284	5,66324E-06	4,583469E-07
24	-1161,87	-1158,31	0,994	-0,427	0,997	0,182	-0,425	9,40079E-06	1,711890E-06
25	-1549,15	-1545,19	0,995	-0,569	0,997	0,324	-0,568	6,52117E-06	2,111102E-06
26	-1936,44	-1936,44	1,000	-0,711	1,000	0,506	-0,711	2,04178E-13	1,032792E-13
Avg	2722,71					Sum	26,094		5,533593E-04
								NMSE	**2,12066E-05**

Table-13. NMSE Performance Index Evaluation for Column Moment at 0° Rotation

No.	Mn PCACOL (kN-m)	Mn CALC (kN-m)	NMSE C_a/C_o	si	ki	si^2	si*ki	$(1-ki)^2$	$si^2 * (1-ki)^2$
1	-17,82	-17,82	1,000	-0,033	1,000	0,001	-0,033	5,38698E-08	5,794950E-11

2	82,76	82,76	1,000	0,152	1,000	0,023	0,152	1,96863E-09	4,567662E-11	
3	187,83	179,76	0,916	0,346	0,957	0,120	0,331	1,84524E-03	2,205322E-04	
4	300,36	293,39	0,954	0,553	0,977	0,306	0,540	5,38047E-04	1,644346E-04	
5	403,90	397,93	0,971	0,743	0,985	0,553	0,732	2,18523E-04	1,207627E-04	
6	498,51	496,11	0,990	0,918	0,995	0,842	0,913	2,31233E-05	1,946640E-05	
7	569,64	567,94	0,994	1,048	0,997	1,099	1,045	8,95632E-06	9,845079E-06	
8	638,54	637,37	0,996	1,175	0,998	1,381	1,173	3,33909E-06	4,612043E-06	
9	698,23	696,68	0,996	1,285	0,998	1,652	1,282	4,90884E-06	8,107085E-06	
10	745,98	744,89	0,997	1,373	0,999	1,885	1,371	2,12280E-06	4,001767E-06	
11	788,77	788,10	0,998	1,452	0,999	2,108	1,451	7,30994E-07	1,540647E-06	
12	827,66	827,32	0,999	1,523	1,000	2,321	1,523	1,65529E-07	3,841207E-07	
13	863,56	863,51	1,000	1,589	1,000	2,526	1,589	3,03216E-09	7,659955E-09	
14	891,06	891,28	1,000	1,640	1,000	2,690	1,640	6,15982E-08	1,656801E-07	
15	880,04	880,56	1,001	1,620	1,001	2,624	1,621	3,53539E-07	9,275350E-07	
16	861,88	862,60	1,002	1,586	1,001	2,516	1,588	6,93529E-07	1,745208E-06	
17	841,63	842,08	1,001	1,549	1,001	2,400	1,550	2,87508E-07	6,898915E-07	
18	819,66	820,15	1,001	1,509	1,001	2,276	1,510	3,58053E-07	8,148973E-07	
19	755,39	756,34	1,003	1,390	1,001	1,933	1,392	1,57663E-06	3,047612E-06	
20	669,53	670,39	1,003	1,232	1,001	1,519	1,234	1,66325E-06	2,525720E-06	
21	575,64	576,39	0,000	1,059	0,000	1,123	0,000	1,00000E+00	1,122511E+0	
22	470,11	470,73	1,003	0,865	1,001	0,749	0,866	1,75202E-06	1,311677E-06	
23	361,17	361,64	1,003	0,665	1,001	0,442	0,666	1,71218E-06	7,565913E-07	
24	251,64	252,10	1,004	0,463	1,002	0,215	0,464	3,27638E-06	7,028174E-07	
25	141,71	142,01	1,004	0,261	1,002	0,068	0,261	4,53683E-06	3,086329E-07	
26	18,94	18,94	1,000	0,035	1,000	0,001	0,035	3,37597E-08	4,102486E-11	
							Sum			1,123078E+00
Avg	543,32							24,897	**NMSE**	**0,045109796**

Table-14. NMSE Performance Index Evaluation for Axial Load at 30° Rotation

No.	Pn PCACOL (kN-m)	Pn CALC (kN-m)	NMSE						
			C_a/C_o	si	ki	si^2	si*ki	$(1-ki)^2$	$si^2 * (1-ki)^2$
1	7295,22	7295,22	1,000	2,679	1,000	7,179	2,679	3,00638E-13	2,158324E-12
2	6930,46	6944,60	1,004	2,545	1,002	6,479	2,551	4,16240E-06	2,696899E-05
3	6565,70	6587,56	1,007	2,411	1,003	5,815	2,419	1,10820E-05	6,444329E-05
4	6200,94	6219,43	1,006	2,277	1,003	5,187	2,284	8,89117E-06	4,611800E-05
5	5836,18	5850,45	1,005	2,144	1,002	4,595	2,149	5,98225E-06	2,748644E-05
6	5471,42	5489,48	1,007	2,010	1,003	4,038	2,016	1,08940E-05	4,399304E-05
7	5106,66	5128,67	1,009	1,876	1,004	3,518	1,884	1,85783E-05	6,535460E-05
8	4741,90	4757,43	1,007	1,742	1,003	3,033	1,747	1,07191E-05	3,251321E-05
9	4377,13	4400,37	1,011	1,608	1,005	2,584	1,616	2,81996E-05	7,288168E-05
10	4012,37	4028,98	1,008	1,474	1,004	2,172	1,480	1,71278E-05	3,719637E-05
11	3647,61	3665,85	1,010	1,340	1,005	1,795	1,346	2,49923E-05	4,485595E-05
12	3282,85	3299,88	1,010	1,206	1,005	1,454	1,212	2,69053E-05	3,911440E-05
13	2918,09	2934,69	1,011	1,072	1,006	1,149	1,078	3,23734E-05	3,718629E-05
14	2553,33	2571,29	1,014	0,938	1,007	0,879	0,944	4,94765E-05	4,351202E-05
15	2188,57	2199,90	1,010	0,804	1,005	0,646	0,808	2,67943E-05	1,731253E-05
16	1823,81	1832,55	1,010	0,670	1,005	0,449	0,673	2,29754E-05	1,030904E-05
17	1459,04	1463,68	1,006	0,536	1,003	0,287	0,538	1,00993E-05	2,900173E-06
18	1094,28	1101,20	1,013	0,402	1,006	0,162	0,404	3,99384E-05	6,451249E-06
19	729,52	737,88	1,023	0,268	1,011	0,072	0,271	1,31216E-04	9,420164E-06
20	364,76	371,92	1,040	0,134	1,020	0,018	0,137	3,85526E-04	6,919349E-06
21	0,00	6,36	0,000	0,000	0,000	0,000	0,000	1,00000E+00	0,000000E+00
22	-387,29	-382,92	0,978	-0,142	0,989	0,020	-0,141	1,27460E-04	2,578955E-06
23	-774,58	-771,23	0,991	-0,284	0,996	0,081	-0,283	1,87455E-05	1,517140E-06
24	-1161,87	-1160,73	0,998	-0,427	0,999	0,182	-0,426	9,70747E-07	1,767738E-07
25	-1549,15	-1549,59	1,001	-0,569	1,000	0,324	-0,569	8,07629E-08	2,614540E-08
26	-1936,44	-1936,44	1,000	-0,711	1,000	0,506	-0,711	0,00000E+00	0,000000E+00
Avg	2722,711					Sum	26,106	6,392358E-04	
								2,44858E-05	

Table-15. NMSE Performance Index Evaluation for Column Moment at 30° Rotation

No.	Mn PCACOL (kN-m)	Mn CALC (kN-m)	NMSE						
			C_a/C_o	si	ki	si^2	si*ki	$(1-ki)^2$	$si^2 * (1-ki)^2$
1	-15,43	-15,43	*1,000*	-0,032	1,000	0,001	-0,032	1,51711E-09	1,595801E-12
2	71,05	71,05	*1,000*	0,149	1,000	0,022	0,149	2,34417E-11	5,228133E-13
3	169,58	165,97	*0,958*	0,356	0,979	0,127	0,349	4,54095E-04	5,769329E-05
4	274,67	269,85	*0,965*	0,577	0,982	0,333	0,567	3,07603E-04	1,025279E-04
5	366,89	362,63	*0,977*	0,771	0,988	0,595	0,762	1,34697E-04	8,010519E-05
6	443,85	440,58	*0,985*	0,933	0,993	0,870	0,926	5,44012E-05	4,734899E-05
7	511,08	509,24	0,993	1,074	0,996	1,154	1,070	1,30121E-05	1,501605E-05
8	566,62	565,09	0,995	1,191	0,997	1,418	1,188	7,26697E-06	1,030783E-05
9	610,47	609,13	0,996	1,283	0,998	1,646	1,280	4,79896E-06	7,901429E-06
10	648,92	647,89	0,997	1,364	0,998	1,860	1,362	2,53387E-06	4,714078E-06
11	679,78	679,11	0,998	1,429	0,999	2,042	1,427	9,63793E-07	1,967660E-06
12	705,74	705,49	0,999	1,483	1,000	2,200	1,483	1,29973E-07	2,860047E-07
13	727,32	727,42	1,000	1,529	1,000	2,337	1,529	1,96737E-08	4,597972E-08
14	743,72	744,11	1,001	1,563	1,001	2,444	1,564	2,71679E-07	6,639034E-07
15	747,98	748,59	1,002	1,572	1,001	2,472	1,573	6,55529E-07	1,620323E-06
16	743,39	744,12	1,002	1,563	1,001	2,442	1,564	9,51493E-07	2,323104E-06
17	725,95	726,69	1,002	1,526	1,001	2,328	1,527	1,03814E-06	2,417123E-06
18	692,75	693,60	1,002	1,456	1,001	2,120	1,458	1,49420E-06	3,168046E-06
19	650,36	651,47	1,003	1,367	1,002	1,869	1,369	2,92013E-06	5,456816E-06
20	589,00	590,36	1,005	1,238	1,002	1,533	1,241	5,35207E-06	8,203172E-06
21	522,40	523,76	0,000	1,098	0,000	1,206	0,000	1,00000E+00	1,205691E+00
22	439,74	440,88	1,005	0,924	1,003	0,854	0,927	6,76383E-06	5,778492E-06
23	347,27	348,16	1,005	0,730	1,003	0,533	0,732	6,61787E-06	3,526004E-06
24	249,62	250,22	1,005	0,525	1,002	0,275	0,526	5,84492E-06	1,609041E-06

25	140,55	140,89	1,005	0,295	1,002	0,087	0,296	5,95534E-06	5,197539E-07
26	16,41	16,41	0,999	0,034	1,000	0,001	0,034	7,72169E-08	9,186698E-11
Avg	475,756					Sum	24,873		1,206054E+00
								NMSE	**0,048488446**

Table-16. NMSE Performance Index Evaluation for Axial Load at 45° Rotation

No.	Pn PCACOL (kN-m)	Pn CALC (kN-m)	NMSE						
			C_a/C_o	si	ki	si^2	si*ki	$(1-ki)^2$	$si^2 * (1-ki)^2$
1	7295,22	7295,23	1,000	2,679	1,000	7,179	2,679	5,68393E-13	4,080581E-12
2	6930,46	6945,46	1,004	2,545	1,002	6,479	2,551	4,68351E-06	3,034536E-05
3	6565,70	6588,47	1,007	2,411	1,003	5,815	2,420	1,20304E-05	6,995796E-05
4	6200,94	6223,36	1,007	2,277	1,004	5,187	2,286	1,30695E-05	6,779083E-05
5	5836,18	5850,92	1,005	2,144	1,003	4,595	2,149	6,37921E-06	2,931035E-05
6	5471,42	5495,15	1,009	2,010	1,004	4,038	2,018	1,88127E-05	7,597085E-05
7	5106,66	5124,74	1,007	1,876	1,004	3,518	1,882	1,25343E-05	4,409298E-05
8	4741,90	4759,85	1,008	1,742	1,004	3,033	1,748	1,43317E-05	4,347085E-05
9	4377,13	4400,73	1,011	1,608	1,005	2,584	1,616	2,90626E-05	7,511215E-05
10	4012,37	4038,85	1,013	1,474	1,007	2,172	1,483	4,35678E-05	9,461582E-05
11	3647,61	3668,37	1,011	1,340	1,006	1,795	1,347	3,24029E-05	5,815643E-05
12	3282,85	3302,07	1,012	1,206	1,006	1,454	1,213	3,42700E-05	4,982106E-05
13	2918,09	2935,09	1,012	1,072	1,006	1,149	1,078	3,39491E-05	3,899619E-05
14	2553,33	2568,57	1,012	0,938	1,006	0,879	0,943	3,56263E-05	3,133147E-05
15	2188,57	2201,66	1,012	0,804	1,006	0,646	0,809	3,57924E-05	2,312640E-05
16	1823,81	1835,75	1,013	0,670	1,007	0,449	0,674	4,28373E-05	1,922109E-05
17	1459,04	1466,17	1,010	0,536	1,005	0,287	0,538	2,39074E-05	6,865352E-06
18	1094,28	1102,39	1,015	0,402	1,007	0,162	0,405	5,49319E-05	8,873163E-06
19	729,52	736,81	1,020	0,268	1,010	0,072	0,271	9,97308E-05	7,159792E-06
20	364,76	370,99	1,034	0,134	1,017	0,018	0,136	2,91325E-04	5,228640E-06
21	0,00	5,64	0,000	0,000	0,000	0,000	0,000	1,00000E+00	0,000000E+00
22	-387,29	-382,37	0,975	-0,142	0,987	0,020	-0,140	1,61108E-04	3,259771E-06
23	-774,58	-771,39	0,992	-0,284	0,996	0,081	-0,283	1,69902E-05	1,375075E-06
24	-1161,87	-1160,13	0,997	-0,427	0,999	0,182	-0,426	2,24115E-06	4,081155E-07
25	-1549,15	-1551,96	1,004	-0,569	1,002	0,324	-0,570	3,29198E-06	1,065715E-06
26	-1936,44	-1936,44	1,000	-0,711	1,000	0,506	-0,711	0,00000E+00	0,000000E+00
Avg	2722,71				Sum		26,117		7,855554E-4
								NMSE	**3,00786E-05**

Table-17. NMSE Performance Index Evaluation for Column Moment at 45° Rotation

No.	Mn PCACOL (kN-m)	Mn CALC (kN-m)	NMSE						
			C_a/C_o	si	ki	si^2	si*ki	$(1-ki)^2$	$si^2 * (1-ki)^2$
1	-12,60	-12,60	1,000	-0,031	1,000	0,001	-0,031	2,40004E-08	2,279613E-11
2	61,25	61,25	1,000	0,150	1,000	0,022	0,150	8,35918E-13	1,876193E-14
3	155,02	151,88	0,960	0,379	0,980	0,144	0,371	4,11057E-04	5,909886E-05
4	244,70	240,83	0,969	0,599	0,984	0,358	0,589	2,50736E-04	8,982261E-05
5	323,53	320,37	0,981	0,791	0,990	0,626	0,784	9,56825E-05	5,991881E-05
6	385,66	383,25	0,988	0,943	0,994	0,890	0,937	3,91578E-05	3,484403E-05
7	441,76	439,88	0,992	1,081	0,996	1,168	1,076	1,81283E-05	2,116562E-05
8	486,87	485,24	0,993	1,191	0,997	1,418	1,187	1,11971E-05	1,587937E-05
9	524,21	522,89	0,995	1,282	0,997	1,644	1,279	6,33286E-06	1,041147E-05
10	553,82	552,85	0,997	1,355	0,998	1,835	1,352	3,04553E-06	5,588581E-06
11	577,33	576,74	0,998	1,412	0,999	1,994	1,411	1,05084E-06	2,095495E-06
12	595,28	595,06	0,999	1,456	1,000	2,120	1,455	1,38219E-07	2,930295E-07
13	609,52	609,64	1,000	1,491	1,000	2,223	1,491	3,93829E-08	8,753565E-08
14	620,90	621,30	1,001	1,519	1,001	2,306	1,520	4,05061E-07	9,342540E-07
15	624,01	624,62	1,002	1,526	1,001	2,330	1,528	9,44903E-07	2,201263E-06
16	620,28	621,04	1,002	1,517	1,001	2,302	1,519	1,50935E-06	3,474290E-06
17	609,52	610,46	1,003	1,491	1,002	2,223	1,493	2,38242E-06	5,295367E-06
18	589,35	590,38	1,003	1,442	1,002	2,078	1,444	3,04398E-06	6,325435E-06
19	564,18	565,19	1,004	1,380	1,002	1,904	1,382	3,22610E-06	6,143491E-06
20	513,80	514,87	1,004	1,257	1,002	1,579	1,259	4,36926E-06	6,900762E-06
21	455,52	456,62	0,000	1,114	0,000	1,241	0,000	1,00000E+00	1,241413E+00
22	389,68	390,74	1,005	0,953	1,003	0,908	0,956	7,43741E-06	6,756770E-06
23	320,86	321,75	1,006	0,785	1,003	0,616	0,787	7,62136E-06	4,694236E-06
24	231,74	232,36	1,005	0,567	1,003	0,321	0,568	7,07532E-06	2,273261E-06
25	130,15	130,46	1,005	0,318	1,002	0,101	0,319	5,59422E-06	5,669293E-07
26	13,40	13,39	0,999	0,033	1,000	0,001	0,033	1,40345E-07	1,507679E-10
Avg	408,84					Sum	24,860		1,241758E+00

CONCLUSION

Based on the accuracy test results from 26 iterations of the neutral axis depth CCC, the computed nominal axial force and nominal bending moment capacities were compared with the results from the PCA-COL program using the NMSE (Normalized Mean Square Error) performance index test. To evaluate the nominal axial capacity of the column against the predictions from PCA-COL, the NMSE indices obtained were: **2.12066E-05**, **2.44858E-05**, and **3.00786E-05**, respectively, for bending angles of **0°**, **30°**, and **45°**. For the evaluation of nominal bending moment capacity against PCA-COL predictions, the NMSE indices obtained were: **0.045109796**, **0.048488446**, and **0.04994925**, for the same respective bending angles. These results indicate that the level of agreement or accuracy between the manual calculation results and those produced by PCA-COL is high, as reflected by the NMSE values approaching zero. This also confirms that the closed polygon method—employing counterclockwise numbering for the exterior boundary points and clockwise numbering for the interior boundaries—is appropriate and effective for calculating the interaction diagrams of reinforced concrete columns with hollow cross-sections.

REFERENCES

[1] A. A. Ibraheem and Y. G. Pronina, "On Optimal Design of Reinforced Concrete Columns Subjected to Combined Biaxial Bending and Axial Load," *Vestnik of Saint Petersburg University, Applied Mathematics, Computer Science, Control Processes*, vol. 18, no. 2, pp. 218–230, 2022.

[2] A. M. A. E. Fattah and H. A. Ahmed, "Partial Confinement Utilization for Rectangular Concrete Columns Subjected to Biaxial Bending and Axial Compression," *Int J Concr Struct Mater*, vol. 11, no. 1, pp. 135–149, Mar. 2017.

[3] A. Al-Ansari, "Simplified Irregular Column Analysis by Equivalent Square Method," *Journal of Structural Engineering & Applied Mechanics*, vol. 2, no. 1, pp. 36–46, 2019.

[4] E. Greulich and F. Francis, "Accurate Polygon Centroid Computation Using ARC/INFO GIS," *Journal of Computing in Civil Engineering*, vol. 9, pp. 88–89, 1995.

[5] A. Ranjbaran, "A Computer Model for the Analysis of Masonry Columns," *Journal of Computers & Structures*, vol. 55, no. 3, pp. 543–551, 1995.

[6] K. H. Kwan and T. C. Liauw, "Computerized Ultimate Strength Analysis of Reinforced Concrete Section Subjected to Axial Compression and Biaxial Bending," *Journal of Computers & Structures*, vol. 21, no. 6, pp. 1119–1127, 1985.

[7] J. Marin, "Computing Columns, Footings and Gates Through Moments of Area," *Comput Struct*, vol. 18, no. 2, pp. 343–349, 1984.

[8] Portland Cement Association (PCA), *PCACOL Strength Design of Reinforced Concrete Column Section*. Skokie, IL, USA: PCA, 1992.

[9] Structurepoint-LLC, "spColumnmanual.pdf."

[10] J. K. Wight, *Reinforced Concrete Mechanics and Design*, Global ed. Edinburgh Gate, Harlow, Essex CM20 2JE, England: Pearson Education Ltd., 2016.

[11] A. A. Poli and C. C. Mario, "On the Use of the Normalized Mean Square Error in Evaluating Dispersion Model Performance," *Atmos Environ*, vol. 27A, no. 15, pp. 2427–2434, 1993.

[12] Badan Standarisasi Nasional (BSN), *SNI-2847-2019 Persyaratan Beton Struktural untuk Bangunan*. Jakarta, Indonesia, 2019.

[13] M. A. Ghoneim and T. E. Mahmoud, *Design of Reinforced Concrete Structures*, vol. 2. Cairo, Egypt: Cairo University, 2008.

[14] Ö. Helgason and V. Valdimar, "Development of a Computer Program to Design Concrete Columns for Biaxial Moments and Normal Force," Sweden, 2010.

[15] R. Hulse and W. H. Mosley, *Reinforced Concrete Design by Computer*. Houndmills, Basingstoke, Hampshire, RG21 2XS, UK: Macmillan Education Ltd., 1986.

[16] T. Sato, I. Shimada, and H. Kobayashi, "A Simple Numerical Method for Biaxial Bending Moment-Curvature Relations of Reinforced Concrete Column Section," *Memoirs of the Faculty of Engineering Osaka City University*, vol. 43, pp. 59–67, 2002.

[17] Badan Pertanahan Nasional (BPN), *Bahan Ajar On The Job Training Penggunaan Alat Total Station*. Direktorat Pengukuran Dasar, Deputi Bidang Survei Pengukuran dan Pemetaan, Badan Pertanahan Nasional Republik Indonesia, 2011.

[18] American Concrete Institute (ACI), *Building Code Requirements for Structural Concrete (ACI 318-19), Commentary on Building Code Requirements for Structural Concrete (ACI 318R-19)*. Farmington Hills, MI, USA: ACI, 2019.